

## PHASE TRANSITIONS IN BINARY MIXTURES

BY A. FULIŃSKI AND M. JURKIEWICZ

Department of Theoretical Chemistry, Institute of Chemistry, Jagellonian University, Cracow\*

*(Received July 8, 1971)*

The equilibrium properties of a two-component mixture are calculated in the so-called one-chain approximation (OCA). OCA consists in retaining only the simplest terms (these represented by one-chain graphs) from every virial coefficient, summing the resulting infinite series, and treating the final formulas as analytic continuations of the original series. No additional assumptions are made here — the properties and structure of the system are determined only by the values of state parameters (temperature, density, and composition), and by the shape of two-particle interactions. The computed quantities are the Helmholtz free energy and pressure (equation of state), and the radial distribution functions. Short-range two-particle interactions of the Lennard-Jones type are chosen here in such a way that the attractive force between unlike particles is weaker than that between like particles, all other particle properties being identical for both species. The formation of two coexistent liquid phases, with limited solubility of one species in the other, is found in a certain region of temperatures and densities. Besides, there is an indication of the existence of the point of equal concentrations (azeotropic point) in the gas-liquid transition.

*1. Introduction*

Very little work has been so far devoted to the microscopic description of many-component fluids. The long-known general formulations of the cluster and virial expansions of distribution functions and of the equation of state (*cf. e. g.* [1]) permit a calculation of lower virial coefficients to be made for multicomponent gases. Apart from that, only some very simplified models of binary mixtures have been developed to the point at which some conclusions might be stated. We may quote here, for example, the model of Gaussian molecules examined by Helfand and Stillinger [2], the Ising model description considered by Heims [3], and a somewhat similar Griffiths' model of  $^3\text{He}-\text{He}^4$  mixtures [4]. Moreover, the semi-guessed equation of state for mixtures of hard spheres has been recently proposed by Boublik [5].

Of the more involved methods, the Percus-Yevick [6] (PY), and hypernetted chain [7] (HNC) approximations have been generalized for many-component systems [8]. These approximations are known to yield satisfactory quantitative agreement with

---

\* Address: Instytut Chemii, Uniwersytet Jagielloński, Kraków, Krupnicza 41, Poland.

experiment (or with a computer experiment) for one-component systems (*cf. e. g.* [9]), and may thus be expected to be able to describe the properties of mixtures as well. However, the PY and HNC approximations for  $n$ -component system [8] require the simultaneous solution of a set of non-linear integral equations for  $n(n+1)/2$  different radial distribution functions, and as far as the authors know, no attempt has yet been made towards a practical calculation of any property of a mixture by means of these methods.

We have recently shown that the so-called one-chain (OC) approximation describes qualitatively the phase transitions and the structure of the condensed phases in one-component systems [10]. This approximation represents the analytic continuation of some simple infinite part (that described by graphs build of one chain only) of the Ursell-Mayer virial expansion [1], and may be considered as an approximation to both HNC and PY approximations<sup>1</sup>. It may be also considered as the first iteration of some other methods — this point will be discussed in the last Section (*cf.* also Refs [10] and [11]). The formulae for the radial distribution functions, free energy, pressure, and other thermodynamical functions in the OC approximation may be also easily obtained for many-component systems [11]. Because these formulae are simple enough for numerical computations (with any form of interparticle interactions), and because they lead to quite sensible (qualitatively) results for one-component systems, it seemed interesting to see how does the OC approximation describe the properties of mixtures.

The purpose of this paper is to present the results of such an investigation. We have examined a binary system with the two-particle interactions chosen in such a way that the attraction between the unlike particles is weaker than the attraction between the like particles, all other properties of the particles of both species being identical. This is perhaps a somewhat simplified situation describing no actual mixture; however, the OC approximation itself is much too simple to yield quantitatively correct results; and thus we may look for the qualitative description only. We have found that, in a certain of temperatures and densities, two coexistent liquid phases appear. Besides, an indication of the existence of the point of equal concentrations in liquid and gaseous phases (the azeotropic point) is also found. These results are presented in Section 4; Sections 2 and 3 contain the OC formulae and the details of the assumed interparticle interactions, while some possibility of the extension of these results towards a more quantitative description is discussed shortly in the last Section.

## 2. OC formulae

A system composed of two different species,  $\alpha$  and  $\beta$ , is considered. The thermodynamical limit of an infinitely large system, and the classical limit (negligible quantum effects) are assumed. The independent intensive bulk parameters are: temperature  $T$ , mean volume per one particle  $v$  (or mean number density  $\rho = 1/v$ ), and the mole fraction (number fraction) of the particles  $\alpha$ ,  $x_\alpha$ ;  $x_\beta = 1 - x_\alpha$ . The particles interact with each other through

<sup>1</sup> OC approximation is described by graphs which are contained also in the HNC and PY approximations. In fact, the OC formulae are equivalent with the first iteration of the HNC integral equation.

the pair potentials  $V_{ij}(r)$  ( $i, j = \alpha, \beta$ ,  $V_{ij} = V_{ji}$ ), where  $r$  denotes the relative distance between a given pair of particles.

The OC approximation [11] leads to the following results for the Helmholtz free energy per particle,  $F$ , pressure (equation of state  $P$ , and the radial distribution functions (RDF)  $g_{ij}(r)$ :

$$\frac{F}{kT} = \frac{F_{id}}{kT} + \frac{B_2}{v} + \frac{v}{4\pi^2} \int_0^\infty dq q^2 \left\{ \ln |M(q)/v^2| + H(q) + \frac{1}{v} [x_\alpha \gamma_{\alpha\alpha}(q) + x_\beta \gamma_{\beta\beta}(q)] \right\}, \quad (1)$$

$$\frac{F_{id}}{kT} = -1 + x_\alpha \ln(x_\alpha \lambda_a^3/v) + x_\beta \ln(x_\beta \lambda_b^3/v), \quad (2)$$

$$B_2 = -\frac{1}{2} [x_\alpha^2 \gamma_{\alpha\alpha}(0) + 2x_\alpha x_\beta \gamma_{\alpha\beta}(0) + x_\beta^2 \gamma_{\beta\beta}(0)], \quad (3)$$

$$M(q) = [v - x_\alpha \gamma_{\alpha\alpha}(q)] [v - x_\beta \gamma_{\beta\beta}(q)] - x_\alpha x_\beta \gamma_{\alpha\beta}^2(q), \quad (4)$$

$$H(q) = \frac{1}{2v^2} [x_\alpha^2 \gamma_{\alpha\alpha}^2(q) + 2x_\alpha x_\beta \gamma_{\alpha\beta}^2(q) + x_\beta^2 \gamma_{\beta\beta}^2(q)], \quad (5)$$

$$\begin{aligned} \frac{P}{kT} = & -\frac{1}{kT} \left( \frac{\partial F}{\partial v} \right)_{T, x_\alpha} = \frac{1}{v} + \frac{B_2}{v^2} - \frac{1}{4\pi^2} \int_0^\infty dq q^2 \{ \ln |M(q)/v^2| + \\ & + [M(q)]^{-1} [v x_\alpha \gamma_{\alpha\alpha}(q) + v x_\beta \gamma_{\beta\beta}(q) + 2x_\alpha x_\beta \gamma_{\alpha\beta}^2(q) - \\ & - 2x_\alpha x_\beta \gamma_{\alpha\alpha}(q) \gamma_{\beta\beta}(q)] - H(q) \}, \end{aligned} \quad (6)$$

$$g_{ij}(r) = \exp \left\{ -\frac{V_{ij}(r)}{kT} + \frac{1}{2\pi^2 r} \int_0^\infty dq q \sin(qr) G_{ij}(q) \right\}, \quad (7)$$

$$\begin{aligned} G_{\alpha\alpha}(q) = & [M(q)]^{-1} \{ x_\alpha x_\beta \gamma_{\alpha\alpha}(q) [\gamma_{\alpha\beta}^2(q) - \gamma_{\alpha\alpha}(q) \gamma_{\beta\beta}(q)] + \\ & + v [x_\beta \gamma_{\alpha\beta}^2(q) + x_\alpha \gamma_{\alpha\alpha}^2(q)] \}, \end{aligned} \quad (8)$$

$$\begin{aligned} G_{\alpha\beta}(q) = & [M(q)]^{-1} \gamma_{\alpha\beta}(q) \{ x_\alpha x_\beta [\gamma_{\alpha\beta}^2(q) - \gamma_{\alpha\alpha}(q) \gamma_{\beta\beta}(q)] + \\ & + v (x_\alpha \gamma_{\alpha\alpha}(q) + x_\beta \gamma_{\beta\beta}(q)) \}, \end{aligned} \quad (9)$$

and  $G_{\beta\beta}(q)$  is given by the exchange of the labels  $\alpha$  and  $\beta$  in Eq. (8). All these quantities are expressed in terms of the temperature-dependent functions  $\gamma_{ij}(q)$ , defined as Fourier

transforms of the Mayer functions:

$$\gamma_{ij}(q) = \frac{4\pi}{q} \int_0^{\infty} dr r \sin(qr) [e^{-V_{ij}(r)/kT} - 1], \quad (10)$$

$k$  denotes here the Boltzmann constant,  $B_2$  is the second virial coefficient of the binary mixture,  $F_{id}$  is the Helmholtz free energy of the ideal gas mixture, and  $\lambda_i = (2\pi h^2/mkT)^{1/2}$  is the thermal de Broglie wavelength,  $m$  being the mass of the particle of species  $i$ .

The integrals in (6) and (7), containing the denominator  $M(q) = M(q; T, v, x_\alpha)$ , are singular in some regions of  $T$ ,  $v$ , and  $x_\alpha$ , and thus are to be interpreted as Cauchy principal values. This interpretation may be justified as follows: the formula (1) represents the sum of the OC graphs of the virial series for the free energy, and may be considered as the analytic continuation of this series beyond its radius of convergence, the latter being determined by the condition

$$|v^2 - M(q)| < 1. \quad (11)$$

When the condition (11) is not fulfilled, the integrand in Eq. (1) is singular at some values of the integration variable  $q$ . However, because this singularity is logarithmic, the integral in Eq. (1) is still convergent. The pressure  $P$  should, in fact, be calculated by the (numerical) differentiation of  $F$  with respect to the volume. When the integrand in  $F$  is non-singular, the order of differentiation over  $v$  and integration over  $q$  may be reversed and we are let to Eq. (6). This is not the case when the condition (11) is not fulfilled; however, the formula (6) may still be used when the integral is taken in the sense of the Cauchy principal value<sup>2</sup>. The integrals in Eqs (7) may be, analogously, taken as their principal values, or may be computed according to the theory of Fourier transforms of distributions (generalized functions) [12]. Both these treatments lead to identical results.

### 3. Intermolecular potentials

All the physics of the considered system is determined in the OC approximation — through Eqs (1)–(10) — by the assumed values of  $T$ ,  $v$ , and  $x_\alpha$ , and by the details of the potentials of interactions between different pairs of particles. We assume here that these interactions are described by potential functions  $V_{ij}(r)$  of the Lennard-Jones type. For simplicity we assume further the interactions between like particles to be identical for both species:

$$V_{\alpha\alpha}(r) = 4\epsilon [(\sigma/r)^{12} - (\sigma/r)^6] \quad (12)$$

<sup>2</sup> These statements may be verified by considering the integrals

$$\int_a^b dx \ln |y-x|, \quad \frac{\partial}{\partial y} \int_a^b dx \ln |y-x| = PP \int_a^b \frac{dx}{y-x},$$

( $a < y < b$ ); the singular parts of the integrals involved in Eqs (1) and (6) are reduced to the above forms by expanding the function  $M(q)$  into a Taylor series around the singular point.

*i.e.*, that both the "particles diameters"  $\sigma$  and the strength of interaction  $\varepsilon$  are the same for  $\alpha$  and  $\beta$  particles. The interaction between unlike particles is assumed to be:

$$V_{\alpha\beta}(r) = 4\varepsilon [(\sigma/r)^{12} - 0.5(\sigma/r)^6], \quad (13)$$

*i.e.*, its repulsive part is the same as for like particles, whereas the attraction between unlike particles is twice weaker.

It is convenient to express all the computed quantities in terms of reduced variables. The following choice is assumed:

$$\begin{aligned} V^* &= v/v_0, & T^* &= kT/\varepsilon, & P &= Pv_0/\varepsilon, \\ b_0 &= 2\pi\sigma^3/3, & x &= r/\sigma, \\ F^* &= F/\varepsilon - x_\alpha \ln(b_0/\lambda_\alpha^3) - x_\beta \ln(b_0/\lambda_\beta^3). \end{aligned} \quad (14)$$

#### 4. Numerical results

##### a. Gas-liquid transition: azeotropy

Let us begin with the examination of the properties of the binary system under consideration from the gas side, decreasing the volume  $V^*$  at constant temperature. Fig. 1 presents the typical behaviour of the isotherms of free energy  $F^*$  and the pressure  $P^*$  vs  $V^*$ , calculated from the OC approximation equations (1) and (6). It is seen that there appears a region of  $V^*$  where  $F^*$  ceases to be concave, and the compressibility  $(\partial P^*/\partial V^*)_{T^*}$  is

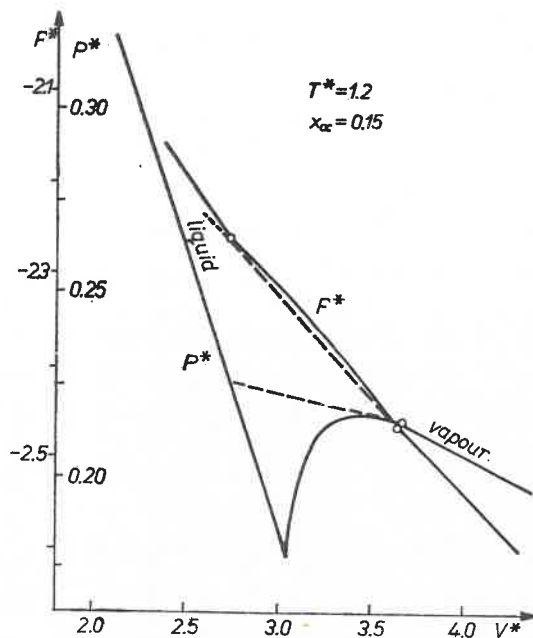


Fig. 1. Free energy,  $F^*$ , and pressure,  $P^*$ , vs the specific volume  $V^*$ , in the OC approximation.  $T^* = 1.2$ ,  $x_\alpha = 0.15$ . The fragments of dashed lines contained between circles show the region of  $V^*$  where the stability condition,  $\delta^2 F > 0$ , is not fulfilled

positive. Such features are commonly interpreted as the indication of the separation of the system into two phases. It was shown [10] that, for one-component system, this transition vanishes at higher temperatures (*i. e.*, the critical point exists), hence we may interpret the medium density phase ( $V^* < 2.7$  in the case presented in Fig. 1) as liquid; further support to this interpretation is given by the shapes of rdf which will be discussed below (*cf.* Figs 6 and 7). The stability condition,  $\delta^2 F > 0$ , leads to the well-known Maxwell construction of the sector of coexisting phases — the dashed lines in Fig. 1. The results for different values of  $x_\alpha$ ,  $V^*$ , and  $T^*$  are collected in Fig. 2, where the phase diagrams are

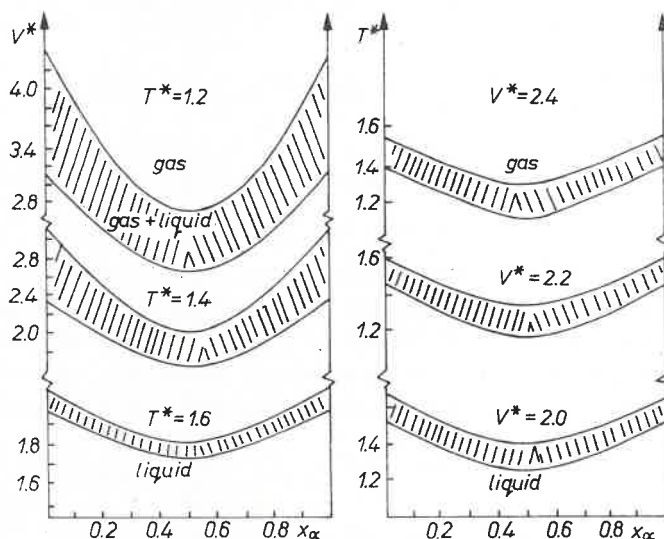


Fig. 2. Phase diagrams for the gas-liquid transition

plotted for the gas-liquid transition. These diagrams show that the condensation of our mixture occurs at lower temperatures and at higher densities than the condensation of a pure substance.

The pressure at which the condensation occurs also depends on the composition of the mixture. The plot of the pressure of the system *vs* concentration, at constant temperature, is given in Fig. 3. The curves labeled  $V^* = 4.2$  and  $V^* = 2.8$  (full lines) are plotted at the constant value of overall volume (of both phases together), and show that the pressure of the system increases when the amount of second substance increases, attaining its maximum value at  $x_\alpha = x_\beta = 0.5$ . The curve  $P^*(x_\alpha)$  at  $V^* = 2.8$  features unstable regions, and points of discontinuity, connected with the gas-liquid transitions. The dashed line in Fig. 3 presents the pressure at which the condensation of the gas mixture of a given composition (at constant  $T^*$  but at different densities) begins (according with the phase diagram of Fig. 2<sup>3</sup>). This diagram possesses one interesting feature:

<sup>3</sup> The dashed line runs, in some parts below the "gas" line at constant volume: this fact shows that the "gas" of a given composition is unstable at this temperature and volume, *i. e.*, that condensation begins at a lower pressure — compare with Fig. 1.

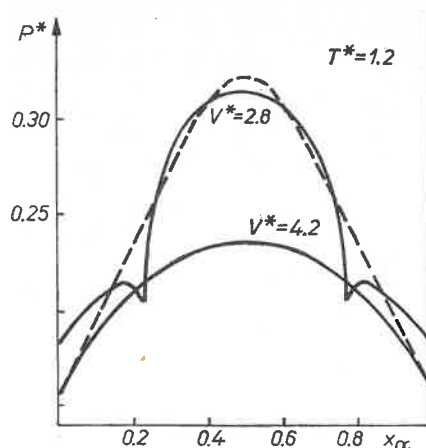


Fig. 3. Pressure  $P^*$  vs the composition of the system. Full lines denote the isochors,  $V^* = 4.2$  and  $2.8$ ; the dashed line shows the pressure at which the condensation of the gas of a given composition begins.  
 $T^* = 1.2$

Let us return for a moment to Fig. 1. The points (densities) at which the gas of a given composition begins and ceases to condense (or the liquid of the same composition begins and ceases to boil) are determined from the shape of the energy  $F^*$  vs  $V^*$ , according to the stability requirements. These points determine, in turn, the values of the pressure  $P_c$  of the condensing gas, and  $P_b$  of the boiling liquid of this composition. These pressures are not equal,  $P_b > P_c$ , which, in agreement with the well-known facts, means that the condensing gas of a given composition  $x_\alpha$  will be in equilibrium with the liquid of another composition,  $x'_\alpha \neq x_\alpha$ , corresponding to the same boiling pressure,  $P'_b = P_c$ . Now, the condensation pressure vs composition,  $P_c(x_\alpha)$  (dashed line in Fig. 3) possesses an extremum (maximum), which is usually connected with the existence of the point of equal concentrations of the vapour and liquid being in mutual equilibrium, *i. e.*, with the phenomenon of azeotropy: the distillation of the liquid (and the condensation of the vapour) of this composition does not lead to the separation of the species. In our case this point corresponds to equal concentrations of both species. In order to prove that the OC approximation predicts indeed the occurrence of the azeotropy phenomenon, the boiling pressure should be also plotted vs composition of the liquid, and in the azeotropic point  $P_c$  should be equal to  $P_b$ . However, more detailed computations are needed (requiring considerable computer time), for a sufficiently exact determination of  $P_b$ .

#### b. Liquid phases: unmixing effect

Let us now look at the properties of our mixture at liquid densities. Fig. 4 shows the dependence of the free energy  $F^*$  on the composition, at constant  $T^*$  and  $V^*$ , for a few values of  $V^*$ . According to the stability conditions, the curves labeled  $V^* = 1.9$  and  $V^* = 1.6$  correspond to the stable system (composed of one phase), whereas the case  $V^* = 1.2$  exhibits instability. Such an instability is usually interpreted as the evidence of the separation of the liquid into two non-miscible liquid phases. The dashed line shows the construc-

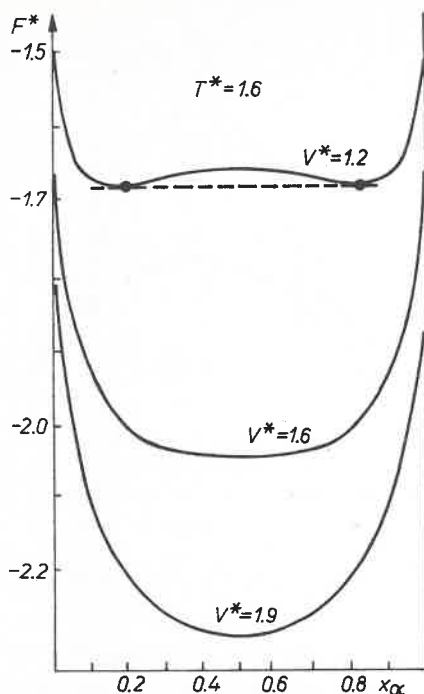


Fig. 4. Free energy  $F^*$  vs composition, in the liquid region.  $T^* = 1.6$

tion of the two-phase region. The results for different values of  $T^*$  and  $V^*$  are collected in Fig. 5 in the form of phase diagrams (isotherms and isochors) to the mixing-unmixing transition. It is seen that the mixture of the substances  $\alpha$  and  $\beta$  in the liquid phase possesses the critical temperature and the critical density of mixing, below which the system separates itself into two liquid phases.

In order to get some insight into the structure of the liquid phases, the rdfs have been computed for the compositions corresponding to one- and two-phase regions. These are shown in Figs 6 and 7, respectively. The full lines, labeled  $N-N$ , denote the average rdf,  $g_{NN}(r)$ , which describes the correlations between all particles, irrespective of the species:

$$g_{NN}(r) = x_\alpha^2 g_{\alpha\alpha}(r) + 2x_\alpha x_\beta g_{\alpha\beta}(r) + x_\beta^2 g_{\beta\beta}(r). \quad (15)$$

In the region of one liquid phase ( $x_\alpha = 0.091$ , Fig. 6) both the  $g_{NN}$  and the rdf of the solvent,  $g_{\beta\beta}$ , exhibit a typical liquid structure: the weak second peak of the second coordination sphere. The rdf of the dissolved species,  $g_{\alpha\alpha}$ , shows a fairly strong clustering of  $\alpha$  particles near a given particle. The most interesting is, however, the rdf for unlike particles,  $g_{\alpha\beta}$ , which demonstrates clearly that indeed we have here the solution of the species  $\alpha$  in the liquid  $\beta$ : the amount of unlike particles around a given particle is above the average homogeneous distribution (the solvation effect)<sup>4</sup>.

<sup>4</sup> According to its definition, the radial distribution function  $g$  describes the correlations between particles:  $g = 1$  means that the particles are distributed homogeneously (at random);  $g \lesssim 1$  means that at a given distance from a given particle there is lower/greater probability of finding a second particle than that resulting from homogeneous distribution.



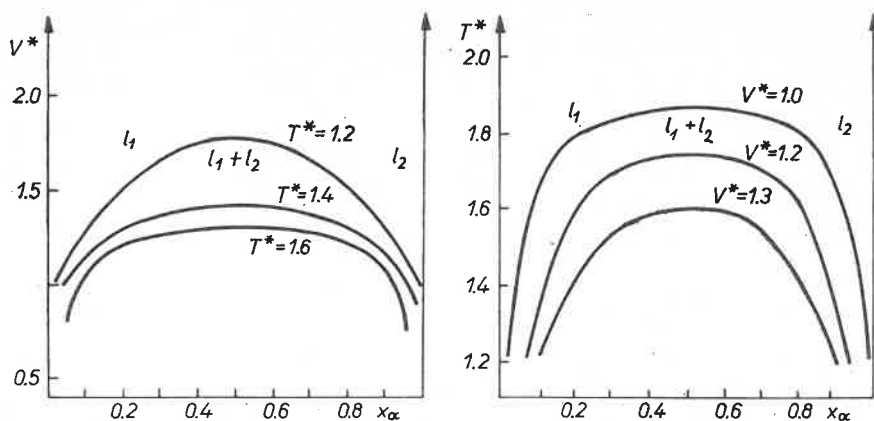


Fig. 5. Phase diagrams for the mixing-unmixing transition.  $l_1$ ,  $l_2$  denote different liquid phases

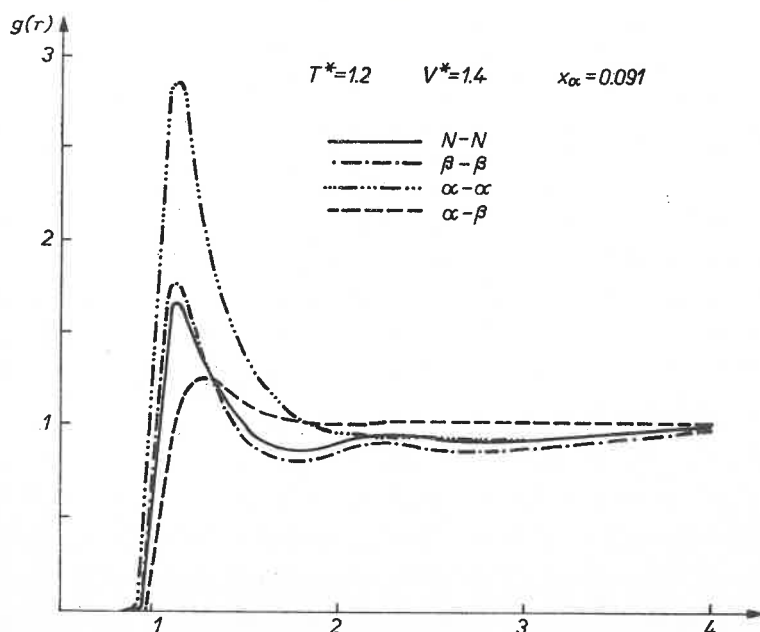


Fig. 6. Radial distribution functions in the one liquid phase region.  $T^* = 1.2$ ,  $V^* = 1.4$ ,  $x_\alpha = 0.091$

A completely reverse situation is seen in the region of concentration ( $x_\alpha = 0.474$ , Fig. 7) interpreted above as the two unmixed liquids phases. First of all, the amount of the unlike particles in the close neighbourhood ( $x = r/\sigma < 2.5$ ) of a given particle is below the average distribution, whereas the correlations between like particles are here fairly strong. Such a picture supports the above interpretation of the existence of two liquid phases with limited solubility of one species in the other.

The second interesting feature is that the situation is reversed for greater interparticle distances ( $x > 2.5$ ): here  $g_{\alpha\beta}$  is above, and  $g_{\alpha\alpha}$  and  $g_{\beta\beta}$  below the homogeneous distribu-

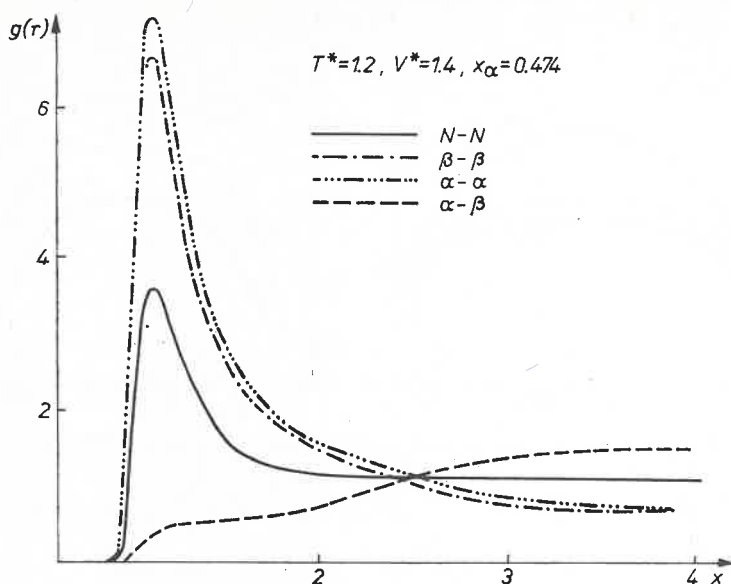


Fig. 7. Radial distribution functions in the region of two liquid phases.  $T^* = 1.2$ ,  $V^* = 1.4$ ,  $x = 0.474$

tion. This results seems to suggest that the average linear extent of a "droplet" of one-phase liquid, given by the OC approximation, is about  $5\sigma$  (at  $T^* = 1.2$ ,  $V^* = 1.4$ ), and that at greater distances we find the second liquid phase. Further, the "droplets" of different phases are distributed rather at random, because  $g_{NN}$ , describing the situation when the differentiation between both species is postponed, shows no structure for greater interparticle distances. This is a gas-like situation, however the existence of the (negative or positive) correlations, when we look at the species, proves that we deal here with the liquid phase.

##### 5. Final remarks

The results presented in this work seem to be physically sensible in the respect that they reproduce correctly the qualitative behaviour of a binary mixture, including the properties of binary liquids. This fact seems to support the reliability of the OC approximation as a relatively simple method of the description of condensed phases. All the physics of the system is determined in this approach by the assumed shapes of intermolecular potentials, and by the values of the state parameters,  $T$ ,  $v$ ,  $x_\alpha$  only. Besides, the knowledge of the free energy as the function of the state parameters permits us to calculate all other thermodynamic functions, whereas the radial distribution functions give at the time an insight into the microscopic structure of the system. The OC approximation — if assumed to be reliable enough — opens thus the possibility of examining the relations between various properties of mixtures, including their microscopic structure, and the characteristics of two-particle interactions, like the strength and range of repulsive and attractive forces, molecular size, etc.

The OC approximation is however able to provide the qualitative characteristics only. Quantitative results might be obtained, for example, by means of the PY or HNC methods: as we have mentioned, OC formulae may be considered as approximate solutions of PY and HNC integral equations. Other generalizations of the OC approximation may be also proposed — the simplest of these is perhaps the following one [11] (*cf.* also Refs [10]):

The quantity

$$W_{ij}(r) = -kT \ln g_{ij}(r)$$

is usually interpreted as the effective potential of interaction between pair of particles,  $i$  and  $j$ , taking into account the influence of all other particles of the system. It seems thus quite sensible to use the quantities  $W_{ij}(r)$ , calculated from Eqs (7) (first OC approximation)

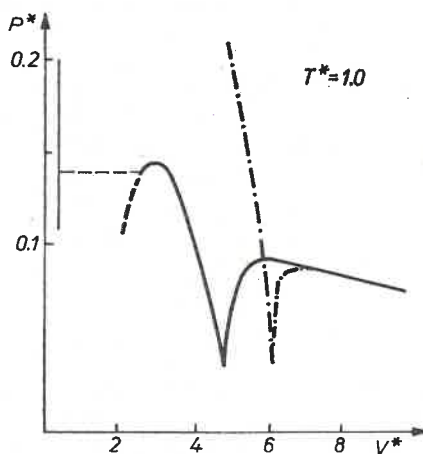


Fig. 8. Comparison of the isotherms  $P^*(V^*)$ , at  $T^* = 1.0$ , for one-component system, in the first (full line) and second (dot-dashed line) OC approximations

in the place of  $V_{ij}(r)$  in Eqs (10), and compute from Eqs (1)–(9), the second OC approximation. This procedure may be repeated recursively until the convergence (if any) is obtained. Such a recursive OC approximation seems to be somewhat simpler than the solution of the sets of PY or HNC nonlinear integral equations. However, the computer (ODRA 1204) being at our disposal is not able to carry out such calculations with sufficient accuracy, mainly because of the principal part integrations involved here. The only result obtained by us is shown in Fig. 8, where the lower-density part of the second OC approximation of the isotherm  $P^*$  vs  $V^*$  is compared with such an isotherm of the first OC approximation, for one-component system with a Lennard-Jones potential, Eq. (12). It is seen that the second approximation shifts the gas-liquid transition towards lower densities (greater  $V^*$ ). The third approximation seems to diminish this effect, but the results are far too inaccurate to be shown here.

## REFERENCES

- [1] J. O. Hirschfelder, C. F. Curtiss, R. B. Bird, *Molecular Theory of Gases and Liquids*, J. Wiley and Sons, Inc., New York 1954; E. Mearon, *J. Chem. Phys.*, **28**, 630 (1958); H. B. Levine, *Phys. Fluids*, **3**, 225 (1960).
- [2] F. H. Stillinger, Jr., E. Helfand, *J. Chem. Phys.*, **41**, 2495 (1964); E. Helfand, F. H. Stillinger, Jr., *J. Chem. Phys.*, **49**, 1232 (1968).
- [3] S. P. Heims, *J. Chem. Phys.*, **45**, 370 (1966).
- [4] R. B. Griffiths, *Phys. Rev. Letters*, **24**, 715 (1970); J. Oitmaa, *Phys. Letters*, **33A**, 230 (1970).
- [5] T. Boublik, *J. Chem. Phys.*, **53**, 471 (1970); H. F. Carnahan, K. E. Starling, *J. Chem. Phys.*, **51**, 635 (1968); **53**, 472 (1970).
- [6] J. K. Percus, G. J. Yevick, *Phys. Rev.*, **110**, 1 (1958).
- [7] J. M. J. Van Leeuven, J. Groeneveld, J. de Boer, *Physica*, **25**, 792 (1959); E. Meeron, *J. Math. Phys.*, **1**, 192 (1960); T. Morita, K. Hiroike, *Progr. Theor. Phys.*, **23**, 1003 (1960).
- [8] K. Hiroike, *Progr. Theor. Phys.*, **24**, 317 (1960); T. Morita, K. Hiroike, *Progr. Theor. Phys.*, **25**, 537 (1961); K. Hiroike, J. Fukui, *Progr. Theor. Phys.*, **43**, 660 (1970); K. Hiroike, T. Morita, *J. Chem. Phys.*, **52**, 5489 (1970).
- [9] J. de Boer, J. M. J. Van Leeuven, J. Groeneveld, *Physica*, **30**, 2265 (1964); D. D. Carley, *Phys. Rev.*, **136**, A127 (1964); *J. Chem. Phys.*, **51**, 3718 (1969); R. O. Watts, *J. Chem. Phys.*, **48**, 50 (1968); **50**, 984, 1358 (1969); M. H. Lee, *Physica*, **43**, 132 (1969).
- [10] A. Fuliński, *Acta Phys. Polon.*, **A37**, 177, 185 (1970); **A39**, 181 (1971); *Phys. Letters*, **31A**, 176 (1970); A. Fuliński, M. Jurkiewicz, *Phys. Letters*, **32A**, 126 (1970); *Acta Phys. Polon.*, **A39**, 167 (1971).
- [11] A. Fuliński, M. Jurkiewicz, *Acta Phys. Polon.*, **A40**, 487 (1971); **A41**, 205 (1972).
- [12] M. J. Lighthill, *Introduction to Fourier Analysis and Generalized Functions*, University Press, Cambridge 1959.